Lecture Notes

Slope Failure

Stefan Hergarten
Institut für Geo- und Umweltnaturwissenschaften
Albert-Ludwigs-Universität Freiburg

Mass Movements
June 2, 2020

1 Yield criteria for elastic media

Elastic behavior is lost at large deformation, where the limit strongly depends on the material. It also depends on the material as well as on temperature whether brittle failure occurs or whether the deformation turns into a ductile type.

Mechanical yield criteria are usually formulated in terms of the stress tensor $\boldsymbol{\sigma}$, although the change in internal structure that is responsible for yield is described by the strain tensor ϵ. The primary reason for preferring stress in this context is that stress can be measured more easily in laboratory experiments than strain. As stress and strain are directly related to each other for elastic media, both descriptions are in principle equivalent.

The generic form of a yield criterion based on stress reads

$$f(\boldsymbol{\sigma}) \;\geq\; f^{\mathrm{crit}} \tag{1}$$

where f is a function of the stress tensor and f^{crit} a threshold value depending on the material.

There are two main types of yield criteria concerning the spatial structure. Anisotropic criteria predict yield at each point taking into account potential failure planes with different orientations explicitly. Such criteria can predict that a material could, e.g., likely break along a horizontal plane for a specific stress tensor, but be stable along a vertical plane.

Isotropic criteria only predict a threshold of failure at each point without being able to predict the most likely orientation of the failure plane. Isotropic criteria are typically used for the transition to ductile behavior. The von-Mises criterion and the Drucker-Prager criterion are the most widely used isotropic yield criteria.

Anisotropic criteria are typically based on the shear stress acting on a potential failure plane. The simplest criterion – named after Henri Tresca – simply assumes that brittle failure occurs if the shear stress exceeds a given, material-dependent threshold. However, the threshold of failure in general increases under compressive normal stress, so that the normal stress acting on the potential failure plane should also be taken into account.

Yield criteria based on shear stress σ_{s} and normal stress σ_{n} can be represented graphically in a Mohr diagram where σ_{s} is plotted vs. σ_{n} (Fig. 1). Normal stress can be considered as a scalar property. In our sign convention, positive normal stresses are tensile, while negative normal stresses are

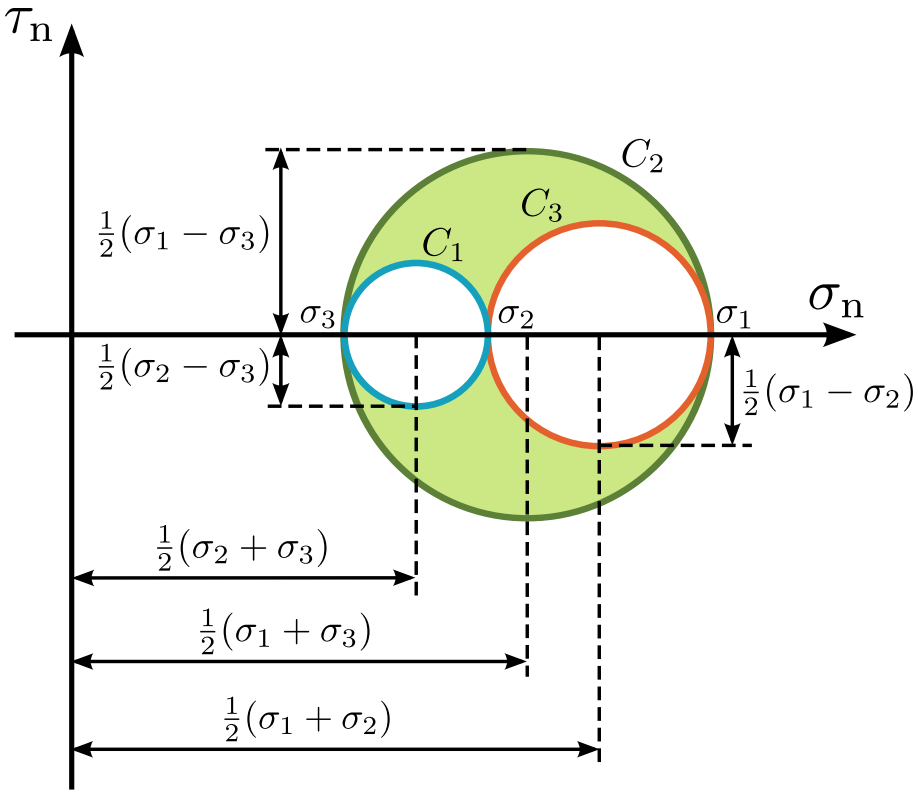

Figure 1: Mohr diagram. The property at the y axis denoted τ_n is the shear stress, σ_s in our notation. Source: Wikipedia.

compressive. Shear stress, however, is a vector in a plane. The Mohr diagram and yield criteria based on shear stress use σ_s as the length of this vector. Consequently, the lower half of the Mohr diagram should not be plotted in 3D considerations. In 2D, however, it would be possible to assign a direction to the shear stress (dextral / sinistral).

The green area between the three circles describes all combinations of σ_n and σ_s that can be achieved by considering planes with different orientations at a given point. Instead of proving this result theoretically, we investigate it in an example in assignment 3. The centers and radii of the three circles are defined by the values of the principal stresses σ_1, σ_2, and σ_3. The notation of Fig. 1 assumes $\sigma_1 \geq \sigma_2 \geq \sigma_3$.

If planes spanned by two of the principal stress directions are considered, the combinations of σ_n and σ_s are on either of the three circles, which is verified by example in assignment 2.

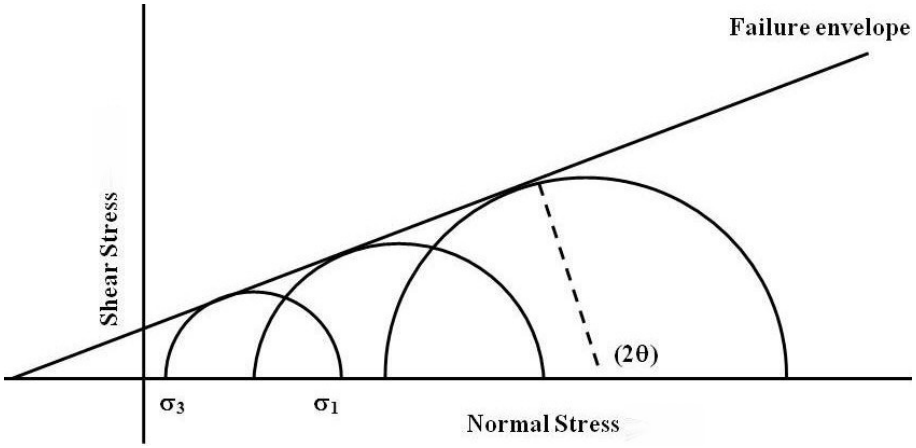

Figure 2: Illustration of the Mohr-Coulomb criterion. The direction to the right corresponds to compressive normal stresses (negative in our sign convention). Source: geohazards.info

2 The Mohr-Coulomb criterion

In the context of slope failure in both bedrock and unconsolidated layers, the Mohr-Coulomb criterion is widely used. It predicts a linear increase of the maximum shear stress σ_s^{crit} that the material can bear with increasing compressive normal stress:

$$\sigma_s^{\text{crit}} = \mp\xi\,\sigma_n + C \tag{2}$$

where our sign convention involves the minus sign (a bit unusual in this context).

The Mohr-Coulomb criterion contains two parameters. The nondimensional coefficient of internal friction ξ is the slope in the Mohr diagram (Fig. 2). It is often expressed as an angle – the angle of internal friction ϕ – according to $\xi = \tan\phi$. The second parameter – the cohesion C – is the intercept with the σ_s axis. It has the same unit as stress (Pa) and describes the shear stress that the material can bear at zero normal stress. Table 1 gives some typical values of C and ϕ.

Table 1: Typical parameter values of the Mohr-Coulomb criterion of materials relevant in the context of mass movements.

	C	ϕ
surface rocks	10 MPa	30–50°
soils	0–100 kPa	20–40°
snow	0–500 Pa	15–30°

3 The factor of safety

The factor of safety (FoS) is a widely used concept in the context of failure and not restricted to mechanical failure. If L is any measure of the actual load and L^{crit} the load where failure occurs, the factor of safety is defined by

$$\text{FoS} = \frac{L^{\text{crit}}}{L}. \tag{3}$$

The factor of safety thus states by which factor the actual load could be increased until failure occurs.

The factor of safety according to the Mohr-Coulomb criterion is

$$\text{FoS} = \frac{\sigma_s^{\text{crit}}}{\sigma_s} = \frac{-\xi\,\sigma_n + C}{\sigma_s}. \tag{4}$$

If FoS ≤ 1 at any point for any orientation, crack formation would be initiated there. Accordingly, we call this definition the local factor of safety in the following.

4 Stability against translational slides

In assignment 1 we computed the stress field in a straight slope with given a slope angle β. This result can be used for estimating the stability of the slope against translational sliding, i. e., against failure along a surface-parallel plane in a given depth. If we use the coordinate system aligned to the slope, the normal vector is $\vec{n} = \begin{pmatrix}0\\0\\1\end{pmatrix}$. Then the normal stress is $\sigma_n = \rho g x_3 \cos\beta$, and the shear stress $\sigma_s = -\rho g x_3 \sin\beta$. The x_3 axis is pointing upward (normal to the surface), so that $x_3 = -h\cos\beta$ where h is the depth below the surface measured normal to the surface (not vertically). Inserting the stresses into Eq. 4 yields

$$\text{FoS} = \frac{\rho g h \tan\phi\,\cos\beta + C}{\rho g h \sin\beta} = \frac{\tan\phi}{\tan\beta} + \frac{C}{\rho g h \sin\beta}. \tag{5}$$

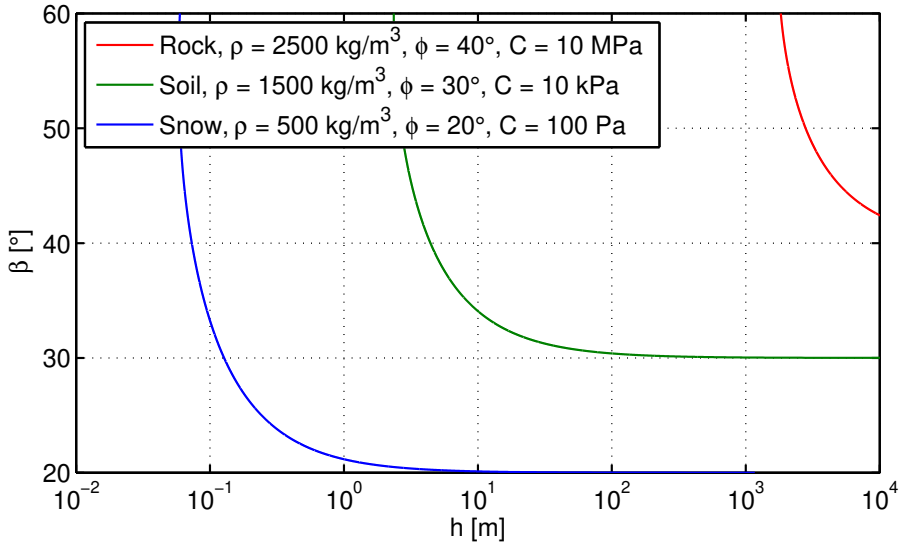

Figure 3: Maximum stable slope angle against translational failure for different materials.

This value is the same along the entire potential slip surface, so that it can also be used as a criterion for the stability of the slope against translational failure.

As an immediate consequence, the slope is stable (FoS > 1) for $\beta < \phi$, i. e., if the slope is less steep than the angle of internal friction. Cohesion results in an increasing factor of safety. Figure 3 shows examples for typical properties of solid rock, soil, and snow. Non-fractured rocks are in principle always stable due to the high cohesion. Typical soils are also quite stable at moderate slope angles. Instability if often triggered by water (see Sect. 10).

According to Eq. 5, the additional stability due to cohesion decreases with depth.

5 Scaling properties

The result that the additional stability due to cohesion decreases with depth is not limited to translational slides. It is a general scaling property of the steady-state version of Cauchy's equations of motion,

$$\mathrm{div}(\boldsymbol{\sigma}) + \rho\vec{g} \;=\; \vec{0} \qquad (6)$$

(in our sign convention).

Let us assume two slopes consisting of the same material and with the same geometry except for a scaling factor f, which means that slope 2 is stretched by a factor f in all directions compared to slope 1. Then the gravitational force $\rho\vec{g}$ is the same in both slopes, and thus also $\mathrm{div}(\boldsymbol{\sigma})$. As the divergence operator consists of first-order spatial derivatives, the stress tensor $\boldsymbol{\sigma}$) in slope 2 must be by the factor f greater than in slope 1. Rescaling the normal stress and the shear stress in Eq. 4 by f yields

$$\mathrm{FoS} \;=\; \frac{-\xi\, f\, \sigma_n + C}{f\, \sigma_s} \;=\; \frac{-\xi\, \sigma_n + \frac{C}{f}}{\sigma_s}. \qquad (7)$$

Thus, the local FoS in slope 2 would (only) be the same as that of slope 1 at each point if the cohesion at slope 2 is by the factor f larger than at slope 1. If the cohesion was the same for both materials, the larger slope would have a lower local FoS at each point.

6 Limit equilibrium models

Failure of solid rock is described by crack propagation, which is a progressive process. Once a small crack has formed, the tips of the crack are exposed to high stresses, so that crack propagation continues. This is in particular relevant for open cracks, i. e., cracks with a tensile component.

Open cracks, however, hardly form in unconsolidated materials under gravity. Local instability will usually result in a shear displacement and thus to some redistribution of shear stress in the neighborhood. However, stability is not fully lost at the location where the displacement occurs; internal friction and cohesion may be almost as high as they were originally. In sum, shear stress is preferably redistributed from domains with a local $\mathrm{FoS} < 1$ to regions with a $\mathrm{FoS} > 1$. So that the local FoS along a potential failure surface becomes more homogeneous. In other words, parts of a potential failure plane with different levels of stability rather support each other than destabilize each other in unconsolidated material.

This leads to the limit equilibrium concept. In principle, limit equilibrium models integrate the actual shear stress and the critical shear stress over a potential slip surface and combine the resulting total forces to an overall FoS.

However, the limit equilibrium concept tends to overestimate the stability.

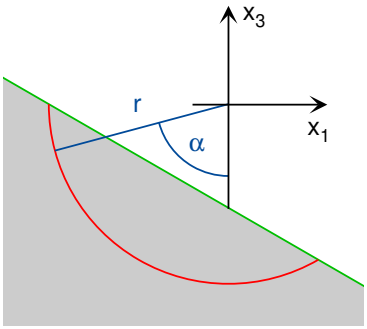

Figure 4: Geometry of a rotational slide in a vertical cross section.

Therefore, engineering applications typically do not use FoS $= 1$ as a strict limit, but define three levels:

FoS $\geq$ 1.3	stable (safe)
$1 <$ FoS < 1.3	conditionally stable
FoS ≤ 1	actively unstable

Parts of the literature use FoS $= 1.5$ instead of 1.3 for the distinction between stable and conditionally stable.

7 Rotational failure

Translational failure considered in Sect. 4 theoretically requires an infinite slope. However, we already learned that the stabilizing effect of cohesion decreases with increases depth, so that other geometries are preferred on slopes of limited size, provided that a sufficient depth to bedrock is available.

In a vertical cross section in direction of potential movement (usually the steepest slope direction), a circular slip surface is preferred to other shapes. It is the only geometry where material can be moved without deforming the displaced body internally. For this reason, simple models of slope instability consider rotational failure in a vertical cross section (Fig. 4).

Models of rotational failure typically express the FoS in terms of torques, also called moments of force. If a force $\vec{F}$ acts at the point $\vec{x}$, the respective torque around the origin is

$$\vec{M} = \vec{x} \times \vec{F}. \tag{8}$$

The total torque acting on the potentially unstable body can be computed in two different ways. First, we can integrate the weight over the volume of the body,

$$\vec{M} = \int \vec{x} \times \rho \vec{g} \, d^3x. \tag{9}$$

Alternatively, we can integrate the stress over the potential failure plane,

$$\vec{M} = \int \vec{x} \times \boldsymbol{\sigma} \vec{n} \, dA, \tag{10}$$

where $\vec{n}$ is the upper normal vector, so that $\vec{x} = -r\vec{n}$, and thus

$$\vec{M} = r \int -\vec{n} \times \boldsymbol{\sigma} \vec{n} \, dA. \tag{11}$$

It we consider a cross section in the x_1-x_3 plane, only the component of $\vec{M}$ normal to this plane, i. e., M_2 is relevant. It is easily recognized that the second component of the term $\vec{n} \times \boldsymbol{\sigma} \vec{n}$ in Eq. 11 equals the shear stress σ_s as defined in assignment 2 (positive to the right, negative to the left). This means that the component of $\vec{M}$ coming out out the paper (opposite to x_2) is

$$M = -M_2 = r \int \sigma_s \, dA, \tag{12}$$

where we call the driving torque $(-M_2)$ M for simplicity.

The calculation of the critical torque M^{crit} where failure occurs is the same,

$$M^{\text{crit}} = r \int \sigma_s^{\text{crit}} \, dA, \tag{13}$$

so that the overall FoS of the limit equilibrium approach is

$$\text{FoS} = \frac{M^{\text{crit}}}{M} = \frac{\int \sigma_s^{\text{crit}} \, dA}{\int \sigma_s \, dA}. \tag{14}$$

The radius r that occurs in both the dominator and the denominator was canceled here.

A small section of the potential failure surface of width w in x_2 direction covering an angle increment $\delta\alpha$ (measured in radians) has a surface area of

$$\delta A = w \, r \, \delta\alpha \tag{15}$$

Thus, the integrals in Eq. 14 can be replaced by integrals of the angle α,

$$\int \ldots \, dA = w \, r \int \ldots \, d\alpha. \tag{16}$$

Alternatively, a coordinate x in horizontal (x_1) direction can be used. It is related to α by

$$x = -r \sin\alpha - \text{const}, \tag{17}$$

so that

$$\frac{dx}{d\alpha} = -r\cos\alpha. \tag{18}$$

As a consequence, the integral over the area can also be expressed in the form

$$\int \ldots dA = wr \int \ldots d\alpha = wr^2 \int \frac{\ldots}{\cos\alpha}\, dx. \tag{19}$$

When calculating the overall FoS, the factors wr and wr^2, respectively, can be canceled, so that

$$\text{FoS} = \frac{\int \sigma_s^{\text{crit}} dA}{\int \sigma_s dA} = \frac{\int \sigma_s^{\text{crit}} d\alpha}{\int \sigma_s d\alpha} = \frac{\int \frac{\sigma_s^{\text{crit}}}{\cos\alpha} dx}{\int \frac{\sigma_s}{\cos\alpha} dx}. \tag{20}$$

For practical calculations, the integrals are replaced by discrete sums, so that

$$\text{FoS} \approx \frac{\sum_i \sigma_{si}^{\text{crit}}\, \delta\alpha_i}{\sum_i \sigma_{si}\, \delta\alpha_i} \approx \frac{\sum_i \frac{\sigma_{si}^{\text{crit}}}{\cos\alpha_i}\, \delta x_i}{\sum_i \frac{\sigma_{si}}{\cos\alpha_i}\, \delta x_i}. \tag{21}$$

8 Fellenius' method

The method introduced by W. Fellenius (1929) was the first model for rotational slope failure taking into account the variation in σ_n and thus σ_s^{crit} along the slip circle. It is still the simplest model in this context. Compared to the continuum mechanics approach considered in detail in assignments 1–5, this method introduces some simplifications that become increasingly relevant at steep slope angles. In turn, it is applicable to arbitrary topographic profiles, while our analytical solution of Cauchy's equations was restricted to the infinite, straight slope.

Fellenius' method was originally developed for a set of discrete vertical slices. For the reason it is often referred to as the ordinary method of slices (OMS). It can, however, also be developed in terms of the stress tensor, which makes it easier to recognized the simplifications.

It was recognized in assignment 1 that the largest component of the stress tensor is approximately $\sigma_{33} \approx -\rho g h$ at moderate slope angles, where h

is the the vertical depth below the surface. Fellenius' method neglects all other stress components, i. e., assumes

$$\boldsymbol{\sigma} = \begin{pmatrix} 0 & 0 & 0 \\ 0 & 0 & 0 \\ 0 & 0 & -\rho g h \end{pmatrix}. \tag{22}$$

If we define the angle α as shown in Fig. 4 and the normal and tangent vectors as in assignment 2,

$$\vec{n} = \begin{pmatrix} \sin\alpha \\ 0 \\ \cos\alpha \end{pmatrix} \quad \text{and} \quad \vec{t} = \begin{pmatrix} \cos\alpha \\ 0 \\ -\sin\alpha \end{pmatrix}, \tag{23}$$

we obtain

$$\sigma_n = -\rho g h \cos^2\alpha \tag{24}$$

$$\sigma_s = \rho g h \cos\alpha \sin\alpha \tag{25}$$

$$\sigma_s^{\text{crit}} = C - \sigma_n \tan\phi = C + \rho g h \cos^2\alpha \tan\phi \tag{26}$$

Then the local factor of safety at each point is

$$\text{FoS}_{\text{loc}} = \frac{\sigma_s^{\text{crit}}}{\sigma_s} = \frac{C + \tan\phi\, \rho g h \cos^2\alpha}{\rho g h \sin\alpha \cos\alpha} = \frac{\tan\phi}{\tan\alpha} + \frac{C}{\rho g h \cos\alpha \sin\alpha}. \tag{27}$$

This expression is almost the same as the FoS against translational sliding (Eq. 5) at the point where the slip circle is parallel to the surface ($\alpha = \beta$). The only difference is the term $\cos\alpha$ in the denominator of the last term. This is however, only a matter of the definition of H. When considering translational sliding in Sect. 4, h was measured normal to the surface, while it is measured vertically here.

The respective overall FoS of the limit equilibrium approach (Eq. 20) is

$$\text{FoS} = \frac{\int \frac{\sigma_s^{\text{crit}}}{\cos\alpha}\, dx}{\int \frac{\sigma_s}{\cos\alpha}\, dx} = \frac{\int \left(\frac{C}{\cos\alpha} + \tan\phi\, \rho g h \cos\alpha\right) dx}{\int \rho g h \sin\alpha\, dx}. \tag{28}$$

The respective version of this equation for discrete slices (Eq. 21) reads

$$\text{FoS} \approx \frac{\sum_i \left(\frac{C}{\cos\alpha_i} + \tan\phi\, \rho g h_i \cos\alpha_i\right) \delta x_i}{\sum_i \rho g h_i \sin\alpha_i\, \delta x_i}. \tag{29}$$

In the literature, this equation is often used for slices of constant width $\delta x_i = \delta x$. The factors δx in the dominator and the denominator can be canceled in this case.

9 Bishop's method

All limit equilibrium models assume that different points of the slip circle support each other by sharing load and strength. This idea is incorporated in the concept of the overall FoS. Fellenius' method – the simplest model in this context – assumes no further interaction between different points at the slip circle or between different slices in a discrete representation.

More elaborate models take such interactions, often called interslice forces, into account. These models typically predict a higher stability than Fellenius' model, i. e., a greater FoS. As a simple example, imagine that the material within the slip circle expands. This will lead to an increase in normal stress at the slip circle and thus to an increase in critical shear stress. Provided that the actual shear stresses do not increase, this will result in an increasing FoS. Climbing between two vertical walls would be another example. Friction climbing is in general only possible as long as the surface is not too steep, but if your feet are in touch with two walls in opposite direction, you could increase the normal force and this the maximum friction force almost arbitrarily.

As discussed in Sect. 7, the FoS against rotational failure is defined as a ratio of torques (Eq. 14). According to Eq. 9, the actual torque that defines the denominator can be calculated from the geometry of the slip circle and from the density pattern (if spatially variable) alone. The stress inside the slip circle and thus also what is considered interslice forces cannot change the actual torque. So the actual torque is the same in all limit equilibrium models. As a consequence, the denominators of the expressions for the FoS will always look like those found for Fellenius' method (Eqs. 28 and 29).

The critical torque, however, depends on the normal stress at the slip circle and can be changed by stresses in the slip circle. So the denominator of the expression for the FoS differs from model to model.

In its original form, the approach introduced by A. W. Bishop (1955) introduced a horizontal force acting on each slice. Neither the balance of forces according to Newton's law nor the balance of torques was taken into account. In order to keep the formalism consistent with the previous considerations, we write Bishop's approach in terms of the stress tensor at the slip circle. Compared to Fellenius' approach (Eq. 22), Bishop's approach

introduces only one additional entry σ_{13} in the stress tensor, so that

$$\boldsymbol{\sigma} = \begin{pmatrix} 0 & 0 & \tau \\ 0 & 0 & 0 \\ 0 & 0 & -\rho g h \end{pmatrix} \tag{30}$$

where τ may be different for different points.

Repeating the considerations of the previous section yields

$$\sigma_n = -\rho g h \cos^2\alpha + \tau \cos\alpha \sin\alpha \tag{31}$$

$$\sigma_s = \rho g h \cos\alpha \sin\alpha + \tau \cos^2\alpha \tag{32}$$

$$\sigma_s^{\text{crit}} = C - \sigma_n \tan\phi = C + \tan\phi \left(\rho g h \cos^2\alpha - \tau \cos\alpha \sin\alpha\right) \tag{33}$$

and thus a local factor of safety of

$$\text{FoS}_{\text{loc}} = \frac{\sigma_s^{\text{crit}}}{\sigma_s} = \frac{C + \tan\phi \left(\rho g h \cos^2\alpha - \tau \cos\alpha \sin\alpha\right)}{\rho g h \cos\alpha \sin\alpha + \tau \cos^2\alpha}. \tag{34}$$

This equation can be rewritten in the form

$$\tau = \frac{C + \tan\phi\, \rho g h \cos^2\alpha - \text{FoS}_{\text{loc}}\, \rho g h \cos\alpha \sin\alpha}{\text{FoS}_{\text{loc}} \cos^2\alpha + \tan\phi \cos\alpha \sin\alpha}. \tag{35}$$

We can now insert this expression for τ into Eqs. 31, 32, and 33 and arrive at expressions for the stresses where FoS_{loc} occurs as an unknown property instead of τ. After bringing the terms to a common denominator and simplifying the results as far as possible, we arrive at

$$\sigma_n = \frac{C \tan\alpha - \text{FoS}_{\text{loc}}\, \rho g h}{\text{FoS}_{\text{loc}} + \tan\phi \tan\alpha} \tag{36}$$

$$\sigma_s = \frac{C + \tan\phi\, \rho g h}{\text{FoS}_{\text{loc}} + \tan\phi \tan\alpha} \tag{37}$$

$$\sigma_s^{\text{crit}} = \frac{C + \tan\phi\, \rho g h}{1 + \frac{\tan\phi \tan\alpha}{\text{FoS}_{\text{loc}}}} \tag{38}$$

At this point it should be taken into account that this stress tensor defined in Eq. 30 is not symmetric. This asymmetry violates the conservation of angular momentum. If we used Eq. 37 for calculating the driving torque in the denominator of the overall FoS, the result would be wrong. However, we already know that this driving torque is the same for all limit equilibrium models, so we can use the expression for σ_s from Fellenius' method (Eq. 25). This leads to an overall factor of safety of

$$\text{FoS} = \frac{\int \frac{\sigma_s^{\text{crit}}}{\cos\alpha}\, dx}{\int \frac{\sigma_s}{\cos\alpha}\, dx} = \frac{\int \frac{C + \tan\phi\, \rho g h}{\cos\alpha + \frac{\tan\phi \sin\alpha}{\text{FoS}_{\text{loc}}}}\, dx}{\int \rho g h \sin\alpha\, dx}. \tag{39}$$

This expression still involves the unknown local factor of safety at the right-hand side. The key point of Bishop's method is to assume that $\mathrm{FoS}_{\mathrm{loc}}$ at the right-hand side is the overall FoS, so that

$$\mathrm{FoS} = \frac{\int \frac{C+\tan\phi\,\rho g h}{\cos\alpha+\frac{\tan\phi\,\sin\alpha}{\mathrm{FoS}}}\,dx}{\int \rho g h\,\sin\alpha\,dx} \approx \frac{\sum_i \frac{C+\tan\phi\,\rho g h_i}{\cos\alpha_i+\frac{\tan\phi\,\sin\alpha_i}{\mathrm{FoS}}}\,\delta x_i}{\sum_i \rho g h_i\,\sin\alpha_i\,\delta x_i}. \tag{40}$$

It is, however, not possible to factor out the term FoS at the right-hand side. So it is not possible to compute the FoS directly. A fixed-point iteration is typically used here. Fixed-point iterations are in general used for solving equations of the type $x = f(x)$ where f is a given function. The idea is to start with a first estimate x_0 and the to compute $x_1 = f(x_0)$, $x_2 = f(x_1)$, $x_3 = f(x_2)$ until the difference between two subsequent values is sufficiently small. This scheme converges rapidly if the function f weakly depends on x, which is the case for Eq. 40. This means that we start with a first estimate of the FoS, e. g., from Fellenius method and insert it into the right-hand side of Eq. 40. This yields an improved estimate of the FoS, which is then inserted into the right-hand side. The procedure converges rapidly here, so usually only a few steps of iteration are required.

We can also compute a local factor of safety for Bishop's method, although it is only useful for illustration. Replacing $\mathrm{FoS}_{\mathrm{loc}}$ by FoS in Eq. 39 does not mean that $\mathrm{FoS}_{\mathrm{loc}}$ is indeed constant. Inserting σ_s^{crit} from Eq. 38 with $\mathrm{FoS}_{\mathrm{loc}} = \mathrm{FoS}$ and σ_s from Fellenius method (Eq. 25) yields

$$\mathrm{FoS}_{\mathrm{loc}} = \frac{\sigma_s^{\mathrm{crit}}}{\sigma_s} = \frac{\frac{C+\tan\phi\,\rho g h}{1+\frac{\tan\phi\,\tan\alpha}{\mathrm{FoS}}}}{\rho g h\,\cos\alpha\,\sin\alpha} = \frac{\frac{C}{\rho g h}+\tan\phi}{\left(\cos\alpha+\frac{\tan\phi\,\sin\alpha}{\mathrm{FoS}}\right)\sin\alpha}. \tag{41}$$

10 The role of water

Water is the most important time-dependent factor in slope stability. The effect of water is twofold. First, it influences the stress tensor and thus σ_n and σ_s. Second, the stability at a given stress may change, i. e., the angle of internal friction ϕ and the cohesion C may change. This will result in changes in the critical shear stress σ_s^{crit} at a given normal stress σ_n.

The immediate effect of water on ϕ is typically small, in particular for soils with little cohesion. The cohesion itself typically decreases with increasing water content, particularly for clayey soils. However, an opposite effect, i. e., an increase of cohesion with increasing water content, was also found in some experiments.

The effect of water on the stress tensor is often stronger than the effect on the parameters ϕ and C. First, the additional weight of the water has to be taken into account. So the density ρ is no longer the density of the dry soil, but has to be replaced by the total density including the water in the pores. A uniform increase in ρ would increase all stresses by the same factor. In Sect. 5 we have learned that the cohesion becomes less relevant if the stresses increase. Thus, an increase in density will result in a lower FoS.

The most important effect, however, arises from the fluid pressure. In order to understand how fluid pressure affects stability, we need some fundamentals of poroelasticity. The concept of poroelasticity was originally developed in the context of hydrocarbon reservoirs, but can be directly applied to slope failure, too. Both the stress tensor $\boldsymbol{\sigma}$ and the strain tensor $\boldsymbol{\epsilon}$ are considered on a macroscopic scale and not as the stress at the surface of individual grains or the deformation of individual grains, respectively.

Starting point of the theory is the inverse form of Hooke's law developed in Sect. 3.7 of the continuum mechanics notes,

$$\boldsymbol{\epsilon} \;=\; \frac{1}{2\mu}\,\boldsymbol{\sigma} - \frac{\lambda}{2\mu(\lambda+\frac{2}{3}\mu)}\,\overline{\sigma}\,\mathbf{1}. \tag{42}$$

This form of Hooke's law describes the strain as a function of the stress. Let us now assume a positive fluid pressure p in the pores. If the stress remains constant, the fluid pressure will cause a macroscopic expansion of the porous medium (while compressing the individual grains). In Sect. 3.6 of the continuum mechanics notes we learned that isotropic compression or expansion can be described by the bulk modulus $K = \lambda + \frac{2}{3}\mu$ according to

$$\overline{\sigma} \;=\; K\,\epsilon_v. \tag{43}$$

If we assume $\overline{\sigma} = -p$ (compressive) and take into account that a positive pressure causes macroscopic expansion, this leads to

$$\epsilon_v \;=\; \frac{p}{K}, \tag{44}$$

and thus

$$\boldsymbol{\epsilon} \;=\; \frac{p}{3K}\,\mathbf{1}. \tag{45}$$

This would, however, only be true if expansion by fluid pressure was the same as contraction under a macroscopic stress. This is not the case in general. In the extreme case of soft grains with a rigid backbone, even the entire effect of the fluid pressure would be accomodated by contraction of

the individual grains. In general, the strain caused by fluid pressure is lower than the strain caused by macroscopic stress. Thus, the bulk modulus K must be replaced by another modulus H with $H \geq K$. Adding the respective term to Eq. 42 yields

$$\boldsymbol{\epsilon} = \frac{1}{2\mu}\boldsymbol{\sigma} - \frac{\lambda}{2\mu(\lambda+\frac{2}{3}\mu)}\overline{\sigma}\,\mathbf{1} + \frac{p}{3H}\,\mathbf{1}. \tag{46}$$

The first two factors satisfy the relation

$$\frac{1}{2\mu} - \frac{\lambda}{2\mu(\lambda+\frac{2}{3}\mu)} = \frac{1}{3(\lambda+\frac{2}{3}\mu)} = \frac{1}{3K}, \tag{47}$$

so that the third factor can be split up into

$$\frac{p}{3H} = p\frac{K}{H}\left(\frac{1}{2\mu} - \frac{\lambda}{2\mu(\lambda+\frac{2}{3}\mu)}\right). \tag{48}$$

Inserting this result into Eq. 46 yields

$$\boldsymbol{\epsilon} = \frac{1}{2\mu}\left(\boldsymbol{\sigma} + \frac{K}{H}p\mathbf{1}\right) - \frac{\lambda}{2\mu(\lambda+\frac{2}{3}\mu)}\left(\overline{\sigma} + \frac{K}{H}p\right)\mathbf{1}. \tag{49}$$

This relation is basically the same as Eq. 42, but with $\boldsymbol{\sigma} + \frac{K}{H}p\mathbf{1}$ instead of $\boldsymbol{\sigma}$. The ratio

$$\alpha = \frac{K}{H} \tag{50}$$

is denoted Biot's parameter. As $H \geq K$, it is in the range $0 \leq \alpha \leq 1$. Biot's parameter quantifies to effect of fluid pressure in relation to the effect of macroscopic stress. For igneous rocks with low porosities, the rock matrix provides a quite rigid backbone, resulting in low values of α in the range between about 0.2 and 0.5. For sandstone it is typically in the range between about 0.6 and 0.9, depending on the porosity. For soils, the structure of the matrix is rather weak compared to the individual grains, so α is close to 1 here.

The stress tensor $\boldsymbol{\sigma}$ and the fluid pressure p are often combined to an effective stress tensor

$$\boldsymbol{\sigma}_{\text{eff}} = \boldsymbol{\sigma} + \alpha\, p\, \mathbf{1}. \tag{51}$$

Equation 49 then reads

$$\boldsymbol{\epsilon} = \frac{1}{2\mu}\boldsymbol{\sigma}_{\text{eff}} - \frac{\lambda}{2\mu(\lambda+\frac{2}{3}\mu)}\overline{\sigma}_{\text{eff}}\mathbf{1}. \tag{52}$$

This means that the effective stress at a given fluid pressure causes the same deformation as the effective stress would cause in absence of fluid pressure. It thus makes sense to assume that failure depends on the effective stress instead of the stress itself.

The difference between $\boldsymbol{\sigma}_{\mathsf{eff}}$ and $\boldsymbol{\sigma}$ is isotropic. Thus, normal stresses change according to

$$\sigma_{\mathsf{n,eff}} \;=\; \sigma_{\mathsf{n}} + \alpha p, \tag{53}$$

so they become by αp less compressive. As a consequence, the critical shear stress is reduced by $\alpha p \tan\phi$, while the actual shear stress is not affected. The reduction in critical shear stress due to the reduction of normal stress is typically the strongest effect of water on slope stability.